

# Highly textured growth of AlN films on sapphire by magnetron sputtering for high temperature surface acoustic wave applications

T. Aubert, M. B. Assouar,<sup>a)</sup> O. Legrani, O. Elmazria, C. Tiusan, and S. Robert

*Institut Jean Lamour, UMR 7198, Nancy University-CNRS, BP 70239, Bd des Aiguillettes, 54506 Vandoeuvre Cedex, France*

(Received 28 May 2010; accepted 10 January 2011; published 31 January 2011)

Piezoelectric aluminum nitride films were deposited onto 3 in. [0001] sapphire substrates by reactive magnetron sputtering to explore the possibility of making highly (002)-textured AlN films to be used in surface acoustic wave (SAW) devices for high temperature applications. The synthesized films, typically 1  $\mu\text{m}$  thick, exhibited a columnar microstructure and a high  $c$ -axis texture. The relationship between the microstructures and process conditions was examined by x-ray diffraction (XRD), transmission electron microscopy, and atomic force microscopy analyses. The authors found that highly (002)-textured AlN films with a full width at half maximum of the rocking curve of less than  $0.3^\circ$  can be achieved under high nitrogen concentration and moderate growth temperature, i.e.,  $250^\circ\text{C}$ . The  $\phi$ -scan XRD reveals the high in-plane texture of deposited AlN films. The SAW devices, based on the optimized AlN films on sapphire substrate, were characterized before and after an air annealing process at  $800^\circ\text{C}$  for 90 min. The frequency response, recorded after the annealing process, confirmed that the thin films were still strong in a high temperature environment and that they had retained their piezoelectric properties. © 2011 American Vacuum Society. [DOI: 10.1116/1.3551604]

## I. INTRODUCTION

During the past 20 years, AlN has attracted considerable attention because of its unique combination of remarkable properties,<sup>1</sup> which make it a serious candidate for high frequency, high power, and high temperature (opto)electronic applications. Actually, AlN has a very high chemical and thermal stability, a high thermal conductivity (about 200 W/m. K), a wide direct band gap of 6.2 eV, a high electrical breakdown voltage, and last but not least, is fully compatible with conventional silicon technology.<sup>2</sup> In the field of surface acoustic wave (SAW) applications, AlN is also very attractive:  $c$ -axis oriented AlN exhibits a relatively good electro-mechanical coupling coefficient of 0.3%,<sup>3</sup> coupled to a very high surface wave velocity of 5700 m/s,<sup>4</sup> which is the highest value among the piezoelectric materials. This last property makes it possible to obtain SAW devices that operate at frequencies as high as 8 GHz.<sup>5</sup>

Conjointly, the use of SAW devices in harsh environments has received a lot of attention recently. Knowing that the conventional piezoelectric substrates such as quartz or lithium niobate cannot be used at high temperature,<sup>6</sup> R&D has focused on a new generation of piezoelectric materials that are stable in these conditions. Now, there is a large consensus on using langasite [ $\text{La}_3\text{Ga}_5\text{SiO}_{14}$  (LGS)] for such purposes. In fact, this material has been extensively studied at high temperatures and it has shown very high stability up to its melting point of  $1473^\circ\text{C}$  along with a great resistance to thermal shock treatment.<sup>7</sup> However, it is also characterized by relatively high acoustic propagation losses (4  $\text{m dB}/\lambda$  at 1 GHz), which dramatically increase with frequency and tem-

perature. This limits its use in wireless configurations at frequencies below 1 GHz for applications at  $500^\circ\text{C}$  and probably much less for higher temperatures.<sup>8</sup> Its low surface acoustic velocity (around 2500 m/s) is another disadvantage for it being used at high frequencies. Thus, the realization of a LGS-based SAW device operating in the 2.45 GHz industrial, scientific, and medical (ISM) band requires a lithographic resolution of about 250 nm, which is below the limits of the current lithography technology used for SAW device fabrication. This limitation is quite a hindrance when trying to reduce the size of antennas for wireless devices. Moreover, it also decreases sensor sensitivity due to it being directly proportional to the operating frequency.

Among all the piezoelectric materials, AlN is probably the only alternative to langasite for high frequency SAW applications at high temperature. AlN films are chemically stable up to  $1040^\circ\text{C}$  in vacuum<sup>9</sup> and  $800^\circ\text{C}$  in air<sup>10</sup> while presenting propagation losses much smaller than langasite.<sup>11</sup> Moreover, besides making it possible to adjust the value of the temperature coefficient of frequency, bilayer structures containing AlN could hypothetically lead to a particularly elegant solution for protecting interdigital transducers (IDTs) from external aggressions by creating substrate-transducer-film structures, which means that the IDTs are sandwiched between the substrate and the AlN thin film and thus naturally protected. This possibility is quite appreciable in view of applications in severe conditions.

Regarding the substrate, [0001] sapphire is a very classical substrate for the deposition of AlN films. The lattice mismatch between  $c$ -oriented AlN and [0001] sapphire being reasonable (13%),<sup>12</sup> it is possible to achieve a highly textured or heteroepitaxial film, which ensures a very good alignment of the  $c$ -axis grains and thus optimized piezoelectric cou-

<sup>a)</sup>Electronic mail: badreddine.assouar@lpmi.uhp-nancy.fr

pling. Moreover, SAW velocities on sapphire being very close to that of AlN and thus rather elevated, it is possible to make AlN/sapphire-based devices that work at frequencies as high as 5 GHz.<sup>11</sup> Several deposition techniques have been applied to produce high-textured AlN films on sapphire, for instance, metal-organic chemical-vapor deposition,<sup>3,11</sup> molecular beam epitaxy,<sup>13</sup> pulsed laser deposition,<sup>14</sup> and magnetron sputtering.<sup>15,16</sup> As concerns the sputtering method, it should be noted that the epitaxial texture has only been obtained at relatively high substrate temperatures, at least 500 °C, with a full width at half maximum (FWHM) of rocking curve value for an (002) AlN diffraction peak close to 0.4°.<sup>17</sup>

In this study, we report on the highly textured deposition of *c*-axis oriented AlN on 3 in. [0001] sapphire substrates by rf magnetron sputtering at a moderate temperature (250 °C), with the aim of it being used in SAW devices withstanding temperatures of at least 800 °C. We investigate using x-ray diffraction (XRD), transmission electron microscopy (TEM), and atomic force microscopy (AFM) the texture of the films versus the process parameters as well as their surface morphology. In the last part of this study, SAW tests in high temperature conditions up to 800 °C were realized to demonstrate the possibility of using an AlN/sapphire structure as a substrate for SAW applications in harsh environments. The reasons for making these devices are, on the one hand, to prove that the piezoelectric quality of the films obtained is good and, on the other hand, to show the behavior of the AlN-based SAW devices under a high temperature environment (800 °C).

## II. EXPERIMENT: AlN GROWTH

AlN thin films were reactively deposited on 3 in. [0001] sapphire wafers from a 99.999% pure aluminum 4 in. target and a 99.999% pure nitrogen and argon gas mixture with a conventional rf magnetron sputtering method. The base pressure in the chamber and its diameter were, respectively,  $2 \times 10^{-7}$  mbar and 45 cm. The distance between the target and the substrate was 8 cm.

In this study, we investigated the effect of the different experimental parameters on the properties of the AlN films. Here, we present only the effect of growth temperature and nitrogen concentration in Ar/N<sub>2</sub> gas mixture on the film properties. The other experimental parameters, i.e., the plasma power and the pressure, were optimized in the first step of this study, so the related results will not be reported here. Two series of AlN samples were synthesized under different growth temperatures and under different nitrogen concentrations in the N<sub>2</sub>/Ar gas mixture (see Table I). The evolution of the properties as functions of both of the experimental parameters studied will be presented and discussed in the next part.

TABLE I. Experimental parameters related to both samples series.

Series 1	Nitrogen (%)	Pressure (mbar)	Temperature (°C)	Power (W)
Sample 1	60	$4 \times 10^{-3}$	150	170
Sample 2	60	$4 \times 10^{-3}$	250	170
Sample 3	60	$4 \times 10^{-3}$	350	170
Sample 4	60	$4 \times 10^{-3}$	500	170
Series 2				
Sample 5	60	$4 \times 10^{-3}$	250	170
Sample 6	80	$4 \times 10^{-3}$	250	170
Sample 7	100	$4 \times 10^{-3}$	250	170

## III. RESULTS AND DISCUSSION

### A. Deposition temperature effect

The first series of AlN samples on 3 in. sapphire wafers was performed at different deposition temperatures, from 150 to 500 °C. The temperature remained stable during the process and was measured and controlled by a proportional-integral-derivative thermocouple system. The other experimental parameters, i.e., pressure, power, and nitrogen concentration, were fixed at  $4 \times 10^{-3}$  mbar, 170 W, and 60% N<sub>2</sub>, respectively (see Table I). These samples only exhibited a strong (002) AlN preferential orientation revealed by a XRD theta–2 theta scan. Figure 1(a) illustrates the wafer mapping of rocking curve measurements carried out for the sample synthesized at 250 °C. To see the evolution of the rocking curve as a function of the position on the wafer more clearly, an X-axis scan of this mapping was plotted in Fig. 1(b) for the different growth temperatures. First of all, in Fig. 1, high (002) crystalline orientation with a FWHM of rocking curve of 0.8°–8.37° as a function of its position on the wafer is observed. Actually, for all the deposition temperatures, a lower FWHM was observed at the edge area of the wafer as compared to the central area. The latter presented a FWHM value varying between 2° and 8.37°, while the edge area gave a value between 0.8° and 2°. This result could be explained by the deposition rate effect, which is different in each of these two areas. The nonuniformity of the deposition rate on the 3 in. wafer was due to the magnetron effect. By thickness measurement, this nonuniformity was determined to be about ~10%. We also note that the lowest FWHM was recorded for the sample realized at 250 °C.

### B. Nitrogen concentration effect

#### 1. Results

The second series of AlN samples on 3 in. sapphire wafers was carried out under different nitrogen concentrations in an Ar/N<sub>2</sub> gas mixture. The other experimental parameters—pressure, power, and growth temperature—were fixed at  $4 \times 10^{-3}$  mbar, 170 W, and 250 °C, respectively. A FWHM rocking curve mapping for the AlN film synthesized under 100% N<sub>2</sub> and an example of a rocking curve measurement are showed on Fig. 2. First, the same

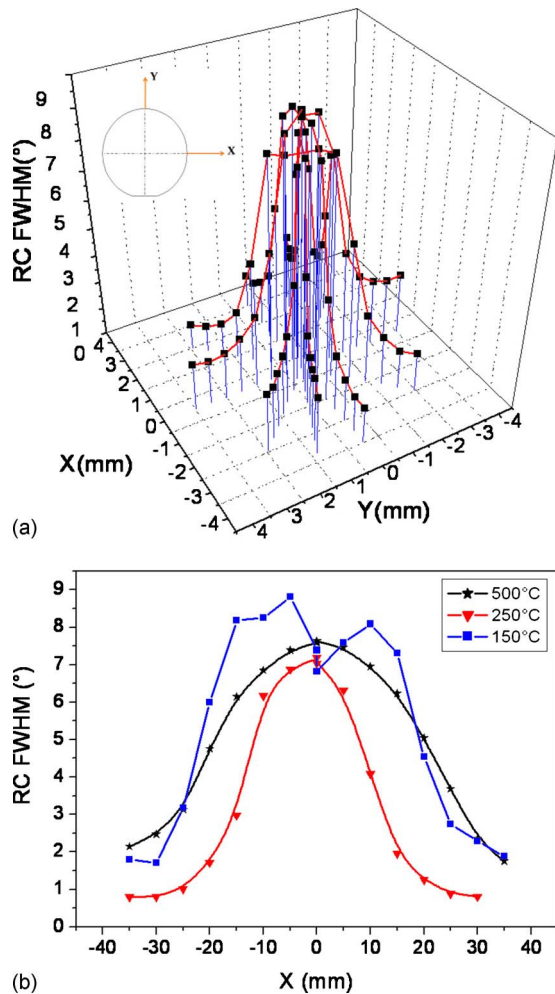


FIG. 1. (Color online) (a) Wafer mapping of the FWHM rocking curve for the sample grown with 60%  $N_2$  and 250 °C. (b) X-axis scan of the FWHM rocking curve mapping under 60%  $N_2$  for different growth temperatures.

behavior as in the first series is observed; a lower FWHM value was obtained at the edge part of the wafer as compared to the central part. Second, very small values and a more homogenous rocking curve FWHM were obtained on the whole of the wafer performed at 100%  $N_2$ . This FWHM value varied between 0.26° and 1.93° on the whole of the wafer, as one can see clearly in Fig. 3, which illustrates a Y-axis scan of the FWHM mapping of all the realized samples. The other samples carried out at 60%  $N_2$  and 80%  $N_2$  also exhibit the same behavior but with higher FWHM. It is worth noting that, for this series, the analyzed AlN/sapphire samples had the same thickness. In fact, the deposition time was adjusted, knowing the growth rate, to obtain the same film thickness (1.5  $\mu\text{m}$ ) for the different  $N_2$  concentrations.

## 2. Discussion

This  $N_2$  series presents two different aspects for discussion. The first one is: why was such a low FWHM rocking curve obtained? Moreover, the second aspect concerns the evolution of the FWHM as a function of the  $N_2$  concentra-

tion in the Ar/ $N_2$  gas mixture. The first aspect can be attributed to the use of [0001] sapphire as a substrate, as well as to the low pressure used in the process, whose value was  $4 \times 10^{-3}$  mbar (optimization of this parameter is not shown in this article). In fact, at such low pressure, the mean free path<sup>18</sup> (6.9 cm in our experimental conditions) of the sputtered atoms becomes comparable with the target-to-substrate distance (8 cm), and hence, they experience less gas phase scattering. The result is that the sputtered Al atoms retain most of their energy when they land on the surface of the growing film.<sup>19,20</sup> They transfer a substantial amount of energy onto the growing film and thus increase the mobility of the adatoms, allowing them to move to the lattice sites toward equilibrium, thus forming a closest-packed (002) plane with the lowest surface energy.

Concerning the second aspect, the effect of the nitrogen concentration, the behavior observed in Fig. 3 can be explained by the peening effect.<sup>19,21–23</sup> At high  $N_2$  concentration, since a N atom is lighter than that of Al, the reflection coefficient of N ions is high enough so that a large fraction of the N ions bombarding the Al target are neutralized and reflected off the target surface immediately upon impact, resulting in additional bombardments of energetic N neutrals onto the growing film. This effect produces a film with a high preferred (002) orientation. On the other hand, the Ar ions are not reflected for the most part since they are heavier than Al. Thus, increased nitrogen concentration favors atomic peening. Both the effects of low pressure and high nitrogen concentration are responsible for the decrease in the FWHM of the rocking curve. These effects are also responsible for the increase in the piezoelectric coefficient because of the concomitant improvement of the crystalline quality of the film.<sup>24</sup>

## C. Characterization of optimized AlN films

Based on the optimization of the AlN film growth, of which only the effects of the deposition temperature and the nitrogen concentration were reported above, the optimized thin films (100%  $N_2$ ,  $4 \times 10^{-3}$  mbar, 170 W, and 250 °C) were characterized mostly in terms of microstructure and morphology by using TEM, AFM, and XRD phi scan. First, the XRD phi-scan measurements reveal that a high in-plane texture was obtained, as illustrated in Fig. 4, presenting the phi scan of (103) planes. Second, TEM analyses confirmed the high texture of optimized films as displayed in Fig. 5. One can actually observe high-textured grains on the film from the TEM image, which is confirmed by the selected area electron diffraction (SAED) pattern attesting to the high crystalline quality of our AlN films. These microstructural analyses that were carried out on the AlN films pointed out the nature of the highly textured growth. The surface morphology was characterized using AFM to determine the surface roughness of the films, which is a very crucial parameter for very low propagation losses. The measurements obtained reveal a homogeneous smooth surface over the whole wafer. Figure 6 shows a three-dimensional (3D) AFM image of the AlN film synthesized at 100%  $N_2$  concentration mapped on

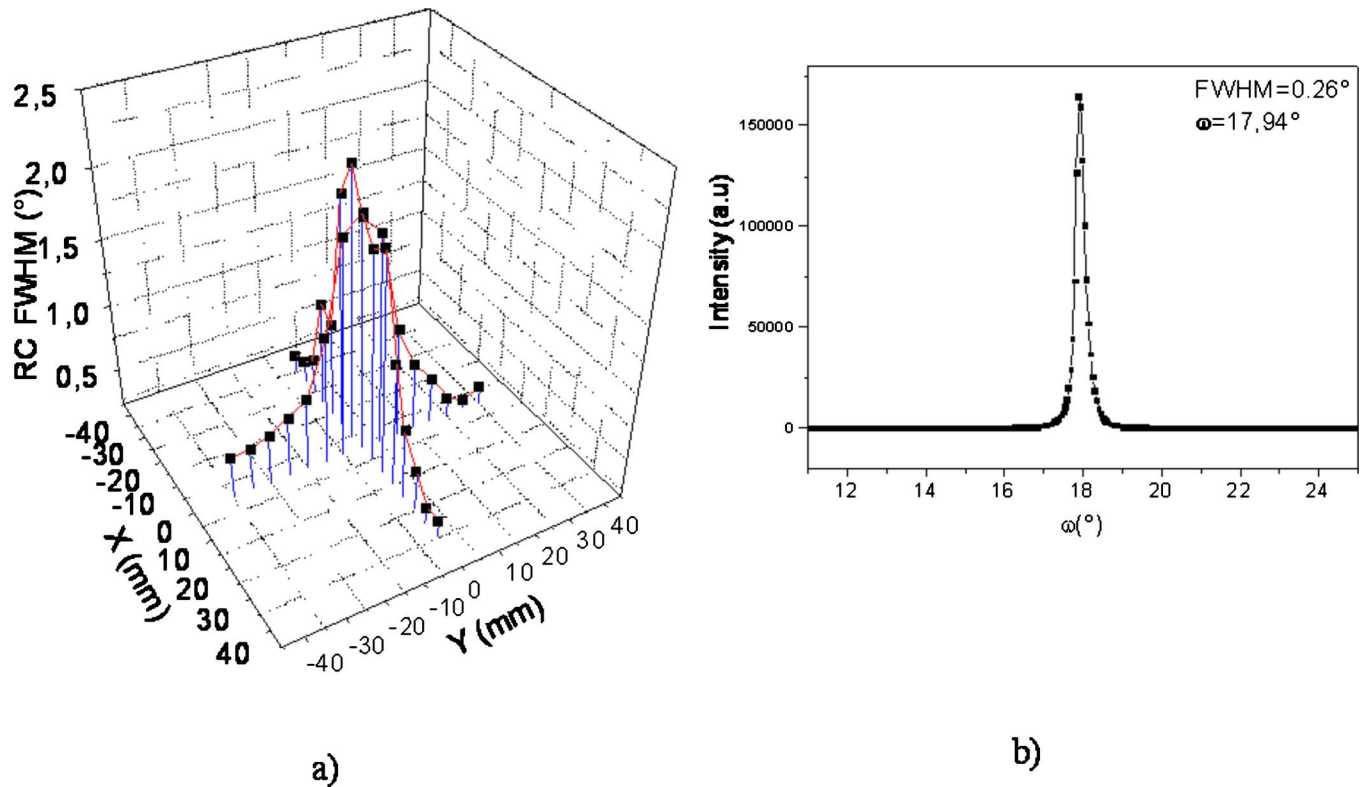


FIG. 2. (Color online) (a) Wafer mapping of the FWHM rocking curve for the sample grown at 100%  $N_2$  and 250 °C. (b) Typical rocking curve obtained at the edge area of the wafer.

the edge of the wafer. The rms roughness was measured at 0.8 nm. This surface roughness is suitable for the targeted SAW application.

#### D. Effect of a high temperature environment on AlN/sapphire structure

To deal with the high temperature characterization of our AlN/sapphire structure, we first carried out structural analyses in the edge area of the wafer (the area presenting the optimal texture) to determine the annealing effect on the AlN

film in terms of the evolution of the preferred orientation and the lattice parameters. Figure 7 shows the rocking curve spectra of the AlN/sapphire structure before and after 800 °C annealing for 90 min. No notable modification concerning the FWHM of rocking curve is recorded. This means that the AlN/sapphire structure withstands this high temperature environment very well and that the (002) preferred orientation of AlN film remains completely intact. The  $c$  parameter of AlN lattice determined from XRD spectra shows that this parameter was conserved before and after annealing, at a value equals to 5.002 Å.

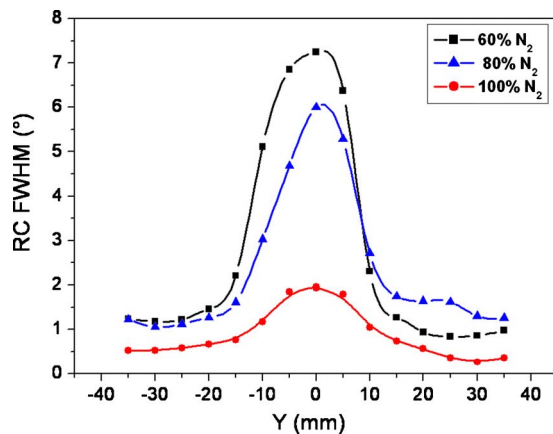


FIG. 3. (Color online) Y-axis scan of the FWHM rocking curve mapping deposited at 250 °C for different nitrogen concentrations in the Ar/ $N_2$  gas mixture.

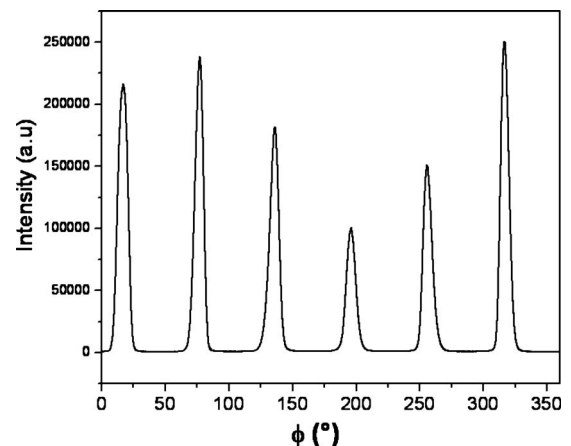


FIG. 4. XRD  $\phi$ -scan of AlN (103) planes for the AlN film grown at 250 °C and 100%  $N_2$ .

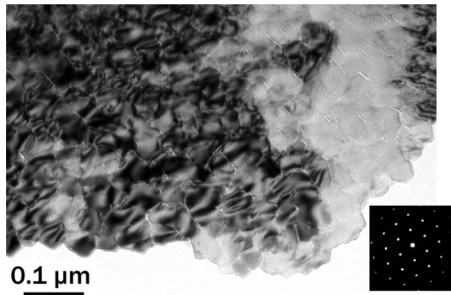


FIG. 5. TEM image and SAED pattern for the AlN film grown at 250 °C and 100% N<sub>2</sub>.

Furthermore, we obtained optical measurements to qualify the optical properties of the AlN film before and after the annealing process. Spectroscopic ellipsometry based on an optical model, which we developed in our previous work,<sup>25</sup> was used to determine the refractive index of these films. The interest of the ellipsometric measurements is that we can, first, have a good idea about the hypothetic formation of an oxide layer on the surface of the AlN film after annealing and, second, have an idea about the thickness of this oxide. Figure 8 presents the variation of the refractive index of the AlN film before and after annealing at 800 °C for 90 min as a function of the wavelength. No significant modification due to annealing can be observed. This means that the optical properties of the AlN film remain intact after annealing and that no significant oxide formation on the top surface of the film was observed. Besides, the refractive index recorded on both AlN/sapphire structures before and after annealing attests to the very high optical quality of the obtained AlN films.

Based on the above characterizations of the AlN films deposited on sapphire substrates, we performed several SAW delay lines with different periods of platinum electrodes, which mean different wavelengths. The device we will show here was made on the edge part of the wafer, i.e., low FWHM of RC. Since the main objective of this study is to point out the ability of an AlN/sapphire structure to operate in a high temperature environment, we will present only the frequency characterization of one of these devices based on a 1.5- $\mu$ m-thick AlN film, with a wavelength of 16  $\mu$ m and 50

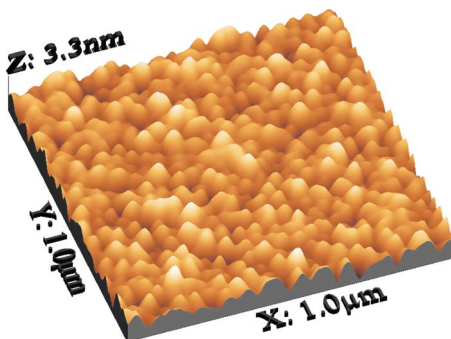


FIG. 6. (Color online) 3D AFM image for the AlN film grown at 250 °C and 100% N<sub>2</sub>.

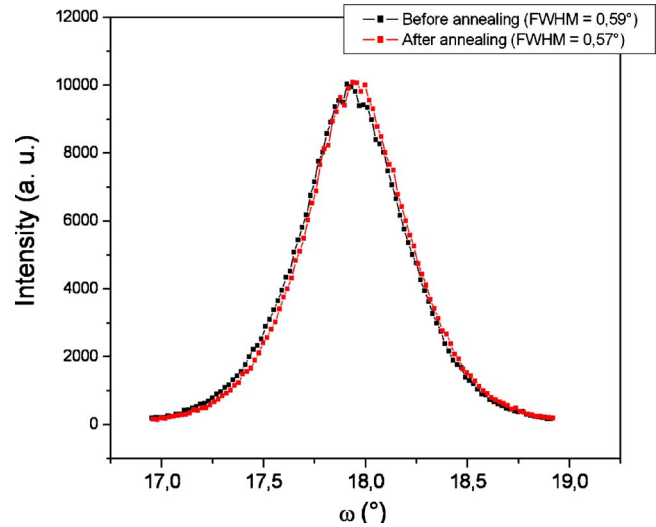


FIG. 7. (Color online) Rocking curves of the AlN/sapphire structures before and after annealing.

pairs of IDTs. This thickness was chosen because it gives a good compromise between a good electromechanical coupling coefficient ( $K^2$ ) and low intrinsic stress in the films. The reasons for making these devices are, on the one hand, to prove that the piezoelectric quality of the films obtained is good and, on the other hand, to show the behavior of the AlN-based SAW devices under a high temperature environment (800 °C). Its frequency responses ( $S_{21}$ ), before and after undergoing high temperature for 90 min, are presented in Fig. 9. The Rayleigh modes at 345 and 343.7 MHz were recorded, respectively, before and after the annealing process. These responses demonstrate good electrical performances, notably in terms of rejection, even though we are not dealing with the optimum thickness of AlN film, which gives the best electromechanical coupling coefficient.<sup>3</sup> This confirms that the crystalline quality of the synthesized AlN films and their high piezoelectric coupling are good. Furthermore, this is further proof of the reliability of our highly textured AlN films under high temperature conditions. In-

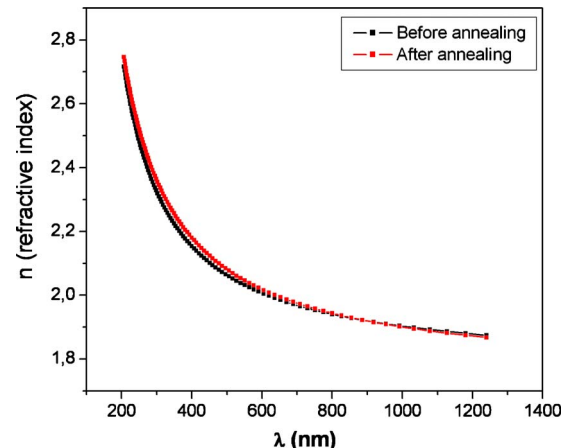


FIG. 8. (Color online) Refractive index dispersion curves of the AlN/sapphire structure before and after annealing.

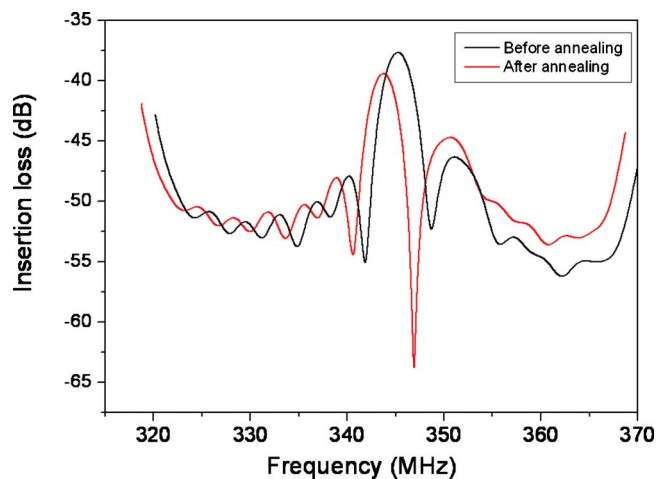


Fig. 9. (Color online) Frequency responses before and after the annealing process of a SAW delay line fabricated on AlN/sapphire structure.

deed, the process of annealing for 90 min at 800 °C under air atmosphere has a very small effect on the frequency response of the device and does not affect the piezoelectric properties of the AlN films. From this result, one can state that the AlN/sapphire-based structure of the SAW devices presented in this study can operate in high temperature environments under air atmosphere up to 800 °C for at least 1 h. This result is capital concerning the use of SAW devices in high temperature environment since it shows that there is a credible alternative to the langasite family, especially for wireless applications in ISM bands over 434 MHz.

#### IV. CONCLUSION

In this article, we have reported on the highly textured growth of AlN films by reactive magnetron sputtering on sapphire substrate at moderate temperature and the reliability of the AlN/sapphire-based structure of SAW devices for high temperature applications. A very low rocking curve FWHM of 0.26° was obtained, demonstrating the highly textured growth of the films deposited at the optimal experimental conditions. The high crystalline quality of our films was confirmed by the TEM and SAED analyses. Their strength in a high temperature environment was proved by XRD and ellipsometry analyses. The AlN/sapphire-based SAW devices were realized and characterized under high temperature in air environment. We have pointed out the reliability of the AlN/

sapphire structure under a temperature of 800 °C for 90 min by the measurements of the frequency responses of SAW based structures before and after the annealing process. Further investigations are currently being realized to determine the limitations of our films in a high temperature environment, in terms of maximum temperature during use as well as the device's lifetime.

- <sup>1</sup>P. Muralt, J. Antifakos, M. Cantoni, R. Lanz, and F. Martin, Proc.-IEEE Ultrason. Symp. 315 (2005).
- <sup>2</sup>C. Caliendo, P. Imperatori, and G. Scavia, Proc.-IEEE Ultrason. Symp. 1614 (2009).
- <sup>3</sup>K. Tsubouchi and N. Mikoshiba, IEEE Trans. Sonics Ultrason. **32**, 634 (1985).
- <sup>4</sup>R. J. Jiménez Riobóo *et al.*, J. Appl. Phys. **92**, 6868 (2002).
- <sup>5</sup>M. B. Assouar, O. Elmazria, P. Kirsch, and P. Alnot, J. Appl. Phys. **101**, 114507 (2007).
- <sup>6</sup>R. Hauser, L. Reindl, and J. Biniash, Proc.-IEEE Ultrason. Symp. 192 (2003).
- <sup>7</sup>M. Pereira da Cunha, R. J. Lad, T. Moonlight, G. Bernhardt, and D. J. Frankel, Proc.-IEEE Ultrason. Symp. 205 (2008).
- <sup>8</sup>R. Fachberger, G. Bruckner, R. Hauser, C. Ruppel, J. Biniash, and L. Reindl, Proc.-IEEE Ultrason. Symp. 1223 (2004).
- <sup>9</sup>O. Ambacher, M. S. Brandt, R. Dimitrov, T. Metzger, M. Stutzmann, R. A. Fisher, A. Miehr, A. Bergmaier, and G. Dollinger, J. Vac. Sci. Technol. B **14**, 3532 (1996).
- <sup>10</sup>J. W. Lee, I. Radu, and M. Alexe, J. Mater. Sci.: Mater. Electron. **13**, 131 (2002).
- <sup>11</sup>K. Uehara, C. M. Yang, T. Shibata, S. K. Kim, S. Kameda, H. Nakase, and K. Tsubouchi, Proc.-IEEE Ultrason. Symp. 203 (2004).
- <sup>12</sup>C. J. Sun, P. Kung, A. Saxler, H. Ohsato, K. Haritos, and M. Razeghi, J. Appl. Phys. **75**, 3964 (1994).
- <sup>13</sup>J. Xu, J. S. Thakur, G. Hu, Q. Wang, Y. Danylyuk, H. Ying, and G. W. Auner, Appl. Phys. A: Mater. Sci. Process. **83**, 411 (2006).
- <sup>14</sup>J. Meinschien, F. Falk, R. Hergt, and H. Stafast, Appl. Phys. A: Mater. Sci. Process. **70**, 215 (2000).
- <sup>15</sup>Y. Huttel, H. Gomez, A. Cebollada, G. Armelles, and M. I. Alonso, J. Cryst. Growth **242**, 116 (2002).
- <sup>16</sup>Q. X. Guo, T. Tanaka, M. Nishio, and H. Ogawa, Vacuum **80**, 716 (2006).
- <sup>17</sup>F. Engelmark, G. F. Iriarte, I. V. Katardjiev, M. Ottosson, P. Muralt, and S. Berg, J. Vac. Sci. Technol. A **19**, 2664 (2001).
- <sup>18</sup>C. J. Adkins, *Equilibrium Thermodynamics* (Cambridge University Press, Cambridge, 1983).
- <sup>19</sup>J. S. Cherng, C. M. Lin, and T. Y. Chen, Surf. Coat. Technol. **202**, 5684 (2008).
- <sup>20</sup>A. Fardeheb-Mammeri, M. B. Assouar, O. Elmazria, J.-J. Fundenberger, and B. Benyoucef, Semicond. Sci. Technol. **23**, 095013 (2008).
- <sup>21</sup>J.-H. Song, S.-C. Wang, J. C. Sung, J.-L. Huang, and D.-F. Lii, Thin Solid Films **517**, 4753 (2009).
- <sup>22</sup>D. W. Hoffman and J. A. Thornton, Thin Solid Films **40**, 355 (1977).
- <sup>23</sup>H. Windischmann, Crit. Rev. Solid State Mater. Sci. **17**, 547 (1992).
- <sup>24</sup>M.-A. Dubois and P. Muralt, J. Appl. Phys. **89**, 6389 (2001).
- <sup>25</sup>T. Easwarakhanthan, M. B. Assouar, P. Pigeat, and P. Alnot, J. Appl. Phys. **98**, 073531 (2005).